Contents

1 Quantum Imaging with Continuous Variables

Luigi A. Lugiato, Alessandra Gatti, and Enrico Brambilla

INFM, Dipartimento di Fisica e Matematica, Universitá dell'Insubria, Via Valleggio 11, 22100, Como, Italy luigi.lugiato@uninsubria.it

1.1 Introduction

A significant fraction of the research activities in the field of quantum imaging concerns optical Parametric Down-Conversion (PDC). Some basic features of this phenomenon will be described in this first chapter of the volume, which deals with the multiphoton regime of the signal–idler field, that one meets in Optical Parametric Amplifiers (OPA) with medium or high gain or in Optical Parametric Oscillators (OPO). In this case, the behavior of the system is naturally described in terms of continuous variables such as field intensity or field quadratures. On the other hand, in the (very) low gain regime of the OPA, one detects coincidences between signal and idler photons and a significant part of the literature on quantum imaging deals with this case, as illustrated in the review article [1].

The first part of this chapter, which is based on the tutorial delivered by one of us (L. A. L.) in the Cargèse workshop,[1] will introduce some key concepts in the continuous variable description, such as squeezing in quadratures and in photon number difference, or entanglement between quadratures, and the basic connection between this entanglement and squeezing. This will be done with the help of two paradigmatic models, one including a single radiation mode and the other with two modes. The second part of this chapter will be devoted to the spatially multimode configuration that one meets in OPAs and in degenerate OPOs. We will discuss the topic of spatially multimode squeezing or local squeezing and of spatial correlations, with the related near-field/far-field interest for quantum imaging, namely the detection of weak amplitude or phase objects duality in type-I OPA/OPO. Then we will turn our attention to two subjects of direct detection beyond the standard quantum limit and the image amplification by parametric down-conversion. The results illustrated in this chapter have been obtained prior to QUANTIM, whereas new results are included in Chapter 2 and Chapter 5.

[1] "Imaging at the Limits," ESF/PESC Exploratory Workshop, *Cargèse (Corsica), France, 5-11 September 2004*.

1.2 The Concepts of Squeezing and of Entanglement with Continuous Variables, and Their Intrinsic Connection

1.2.1 Prototype Model I

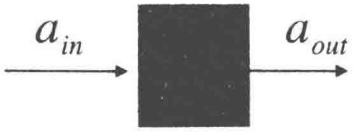

Fig. 1.1. "Input-output box" for an OPA (or an OPO below threshold) in the degenerate single-mode configuration.

Let us consider the "black box" in Fig. 1.1, with an input mode and an output mode associated with annihilation and creation operators $\hat{a}_{\rm in}$ and $\hat{a}_{\rm in}^{\dagger}$ and $\hat{a}_{\rm out}$, $\hat{a}_{\rm out}^{\dagger}$, respectively, with

$$\left[\hat{a}_{\rm in}, \hat{a}_{\rm in}^{\dagger}\right] = 1 \,, \qquad \left[\hat{a}_{\rm out}, \hat{a}_{\rm out}^{\dagger}\right] = 1 \,. \tag{1.1}$$

Let us assume the input-output relation

$$\hat{a}_{\rm out} = U\hat{a}_{\rm in} + V\hat{a}_{\rm in}^{\dagger}, \tag{1.2}$$

with coefficients U and V obeying the condition

$$|U|^2 - |V|^2 = 1, \tag{1.3}$$

which ensures the unitarity of transformation (1.2). In the following we take for definiteness

$$U = \cosh g \,, \qquad V = \sinh g \,. \tag{1.4}$$

A concrete realization of (1.2) is given, for example, by a degenerate OPA (or OPO below threshold) in the single-mode configuration.

Case 1

If $\hat{a}_{\rm in}$ is in a coherent state $\mid \alpha\rangle$, so that the mean value of $\hat{a}_{\rm in}$ is $\langle \hat{a}_{\rm in}\rangle = \alpha$, one has from (1.2)

$$\langle \hat{a}_{\rm out}\rangle = U\alpha + V\alpha^* \,. \tag{1.5}$$

Hence the system behaves as a phase-sensitive amplifier/deamplifier; for example, if α is real one has amplification:

$$|\langle \hat{a}_{\rm out}\rangle|^2 = |U+V|^2\,|\alpha|^2 = \mathrm{e}^{2g}\,|\langle \hat{a}_{\rm in}\rangle|^2 \,, \tag{1.6}$$

whereas if α is imaginary one has deamplification:

$$|\langle \hat{a}_{\rm out}\rangle|^2 = |U-V|^2\,|\alpha|^2 = \mathrm{e}^{-2g}\,|\langle \hat{a}_{\rm in}\rangle|^2 \,. \tag{1.7}$$

Case 2

Let us focus, instead, on the case that $\hat{a}_{\rm in}$ is in the vacuum state $\mid 0\rangle$. If we consider the quadrature components of the input and output modes

$$\hat{X}_{\rm in} = \frac{\hat{a}_{in} + \hat{a}^{\dagger}_{\rm in}}{2} , \qquad \hat{Y}_{\rm in} = \frac{\hat{a}_{\rm in} - \hat{a}^{\dagger}_{\rm in}}{2{\rm i}} , \tag{1.8}$$

$$\hat{X}_{\rm out} = \frac{\hat{a}_{out} + \hat{a}^{\dagger}_{\rm out}}{2} , \qquad \hat{Y}_{\rm out} = \frac{\hat{a}_{out} - \hat{a}^{\dagger}_{\rm out}}{2{\rm i}} , \tag{1.9}$$

the input-output relation (1.2) can be rephrased in the following form,

$$\hat{X}_{\rm out} = {\rm e}^{g} \hat{X}_{\rm in} , \qquad \hat{Y}_{\rm out} = {\rm e}^{-g} \hat{Y}_{\rm in} , \tag{1.10}$$

hence the quadrature component $\hat{X}$ is amplified whereas the quadrature component $\hat{Y}$ is deamplified, and from Fig. 1.2 one sees that the input vacuum state is transformed into a squeezed vacuum state, with squeezing in the quadrature component $\hat{Y}$. By varying the phase of the coefficients U and V with respect to the choice (1.4), the squeezing can be produced in an arbitrary quadrature component $\hat{X}_{\theta} = 1/2(\hat{a}{\rm e}^{-{\rm i}\theta} + \hat{a}^{\dagger}{\rm e}^{{\rm i}\theta})$, for any value of θ.

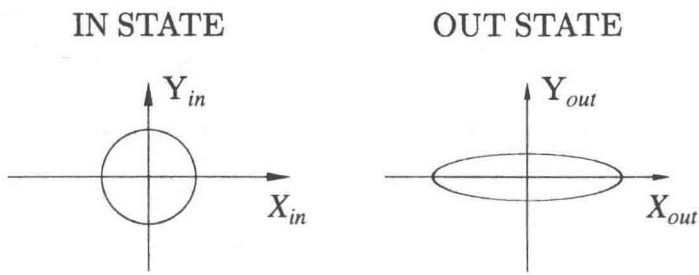

Fig. 1.2. The input-output relation (1.2) with (1.4) transforms the vacuum state into a squeezed vacuum state, with squeezing in the quadrature component $\hat{Y}$.

1.2.2 Prototype Model II

Let us now consider the black box in Fig. 1.3, with two input and two output modes such that

$$\left[\hat{a}_{i,\rm in}, \hat{a}^{\dagger}_{j,\rm in}\right] = \delta_{ij} , \qquad \left[\hat{a}_{i,\rm out}, \hat{a}^{\dagger}_{j,\rm out}\right] = \delta_{ij} \qquad (i,j = 1,2) , \tag{1.11}$$

and the input-output relations

$$\hat{a}_{1\text{out}} = U_1 \hat{a}_{1\text{in}} + V_1 \hat{a}^{\dagger}_{2\text{in}} ,$$
$$\hat{a}_{2\text{out}} = U_2 \hat{a}_{2\text{in}} + V_2 \hat{a}^{\dagger}_{1\text{in}} , \tag{1.12}$$

with the unitarity condition

$$|U_i|^2 - |V_i|^2 = 1 , \qquad U_1 V_2 = U_2 V_1 . \tag{1.13}$$

In the following we take for definiteness

$$U_1 = U_2 = U = \cosh g , \qquad V_1 = V_2 = V = \sinh g . \tag{1.14}$$

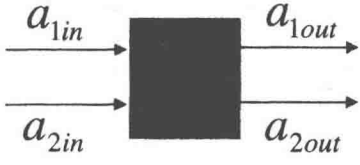

Fig. 1.3. Input-output box for an OPA (or an OPO below threshold) in the nondegenerate two-mode configuration.

A realization of (1.14) is given by a nondegenerate OPA (or OPO below threshold) in the two-mode regime.

Case 1

Let us consider the case when the mode $\hat{a}_{1\text{in}}$ is in a coherent state $|\,\alpha\rangle$, whereas the mode $\hat{a}_{2\text{in}}$ is in the vacuum state $|\,0\rangle$. One obtains from (1.12)

$$\langle \hat{a}_{1\text{out}} \rangle = U_1 \alpha, \qquad \langle \hat{a}_{2\text{out}} \rangle = V_2 \alpha^*, \tag{1.15}$$

so that

$$|\langle \hat{a}_{1\text{out}} \rangle|^2 = (\cosh^2 g)\, |\alpha|^2 = (\cosh^2 g)\, |\langle \hat{a}_{1\text{in}} \rangle|^2 , \tag{1.16}$$
$$|\langle \hat{a}_{2\text{out}} \rangle|^2 = (\sinh^2 g)\, |\alpha|^2 = (\sinh^2 g)\, |\langle \hat{a}_{2\text{in}} \rangle|^2 . \tag{1.17}$$

Hence mode 1 is amplified in a phase-insensitive way, whereas mode 2 is generated from the vacuum, and in the large-gain limit, $g \to \infty$, it becomes equally as strong as mode 1.

Case 1′

Let us assume that both modes $\hat{a}_{1\text{in}}$ and $\hat{a}_{2\text{in}}$ are in the same coherent state $|\,\alpha\rangle$. In this case one has from (1.12), (1.14),

$$\langle \hat{a}_{1\text{out}} \rangle = \langle \hat{a}_{2\text{out}} \rangle = \cosh g\alpha + \sinh g\alpha^* , \tag{1.18}$$

so that as in (1.5), one has a phase-sensitive amplification/deamplification. One can prove that, in general, phase-insensitive amplification degrades the signal-to-noise ratio at least by a factor 2, whereas phase-sensitive amplification can preserve the signal-to-noise ratio (noiseless amplification) [1].

Case 2

Let us consider the case when both $\hat{a}_{1\text{in}}$ and $\hat{a}_{2\text{in}}$ are in the vacuum state. The most interesting situation is in the limit of large g, in which $U_i \approx V_i \approx \mathrm{e}^g/2$ $(i = 1, 2)$, so that by indicating $U = \mathrm{e}^g/2$ relations (1.12) reduce to

$$\begin{aligned} \hat{a}_{1\text{out}} &= U\hat{a}_{1\text{in}} + U\hat{a}^\dagger_{2\text{in}} , \\ \hat{a}_{2\text{out}} &= U\hat{a}_{2\text{in}} + U\hat{a}^\dagger_{1\text{in}} , \end{aligned} \tag{1.19}$$

hence by introducing the quadrature components of the input-output modes

$$\hat{X}_{j,\text{in}} = \frac{\hat{a}_{j,\text{in}} + \hat{a}^\dagger_{j,\text{in}}}{2} , \qquad \hat{Y}_{j,\text{in}} = \frac{\hat{a}_{j,\text{in}} - \hat{a}^\dagger_{j,\text{in}}}{2\mathrm{i}} , \qquad j = 1, 2, \tag{1.20}$$

$$\hat{X}_{j,\text{out}} = \frac{\hat{a}_{j,\text{out}} + \hat{a}^\dagger_{j,\text{out}}}{2} , \qquad \hat{Y}_{j,\text{out}} = \frac{\hat{a}_{j,\text{out}} - \hat{a}^\dagger_{j,\text{out}}}{2\mathrm{i}} \qquad j = 1, 2,$$

one obtains the relations

$$\hat{X}_{2\text{out}} = \hat{X}_{1\text{out}} , \qquad \hat{Y}_{2\text{out}} = -\hat{Y}_{1\text{out}} . \tag{1.21}$$

Therefore, if one measures, for example, $\hat{X}_{1\text{out}}$ and $\hat{Y}_{1\text{out}}$, one can immediately infer the values of $\hat{X}_{2\text{out}}$ and $\hat{Y}_{2\text{out}}$. This is precisely the phenomenon of *quantum entanglement*, and this is completely identical to the original Einstein–Podolsky–Rosen paradox [2], which was formulated for the position x and momentum p of two particles. This formulation of the EPR paradox for continuous variables $\hat{X}$ and $\hat{Y}$ (quadrature components) of two radiation modes was introduced in [3] taking into account the uncertainties in the measurements of $\hat{X}$ and $\hat{Y}$. This was experimentally verified in [4].

1.3 Intrinsic Relation Between Squeezing and Entanglement

In this section we show that there is a basic connection between the two paradigmatic models just discussed, which amounts to an intrinsic relation between entanglement and squeezing.

Let us consider a 50/50 beamsplitter (Fig. 1.4). One demonstrates that:

— If $\hat{a}_1$ and $\hat{a}_2$ are EPR entangled beams (in the sense defined before) then the beam $\hat{b}_1$ is squeezed in the $\hat{Y}$ quadrature and the beam $\hat{b}_2$ is squeezed in the $\hat{X}$ quadrature.

— And vice versa.

Proof

Let us consider the input-output relations of the beamsplitter

$$\hat{b}_1 = \frac{\hat{a}_1 + \hat{a}_2}{\sqrt{2}} , \qquad \hat{b}_2 = \frac{\hat{a}_2 - \hat{a}_1}{\sqrt{2}} . \tag{1.22}$$

Next, let us assume that $\hat{a}_1$ and $\hat{a}_2$ are the entangled output modes $\hat{a}_{1\text{out}}$ and $\hat{a}_{2\text{out}}$ of model II, so that

$$\begin{aligned} \hat{a}_1 &= U\hat{a}_{1\text{in}} + V\hat{a}^\dagger_{2\text{in}} , \\ \hat{a}_2 &= U\hat{a}_{2\text{in}} + V\hat{a}^\dagger_{1\text{in}} , \end{aligned} \tag{1.23}$$

where $\hat{a}_{1\text{in}}$ and $\hat{a}_{2\text{in}}$ are in the vacuum state. By inserting (1.23) into (1.22) we obtain

$$\hat{b}_1 = U\hat{f}_1 + V\hat{f}^\dagger_1, \tag{1.24}$$

$$\hat{b}_2 = U\hat{f}_2 - V\hat{f}^\dagger_2, \tag{1.25}$$

where modes $\hat{f}_1$ and $\hat{f}_2$ are defined as

$$\hat{f}_1 = \frac{\hat{a}_{1\text{in}} + \hat{a}_{2\text{in}}}{\sqrt{2}} , \qquad \hat{f}_2 = \frac{\hat{a}_{2\text{in}} - \hat{a}_{1\text{in}}}{\sqrt{2}} . \tag{1.26}$$

Because $\hat{a}_1$ and $\hat{a}_2$ are in the vacuum state, the same is true for $\hat{f}_1$ and $\hat{f}_2$. Now one notes immediately that (1.24) is identical to the prototype model I (1.2), hence we can conclude that $\hat{b}_1$ is squeezed with respect to the $\hat{Y}$ quadrature. On the other hand, one sees that (1.25) has the same form of

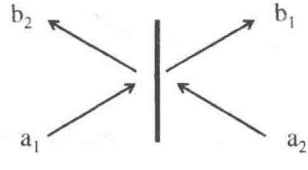

Fig. 1.4. A 50/50 beamsplitter converts modes a_1 and a_2 into modes b_1 and b_2.

model I (1.2) except that V is replaced by $-V$. One can easily prove that this feature implies that $\hat{b}_2$ is squeezed with respect to the $\hat{X}$ quadrature.

1.4 Spatially Multimode Parametric Down-Conversion: Some Topics in Quantum Imaging

1.4.1 Spatially Multimode Versus Single-Mode Squeezing: Optical Parametric Down-Conversion of Type-I

In almost all literature on squeezing one considers single-mode squeezing. If one wants to detect a good level of squeezing, the local oscillator must be matched to the squeezed spatial mode and, in addition, it is necessary to detect the whole beam. If one detects only part of the beam, the squeezing is immediately degraded, because a portion of a mode necessarily involves higher-order modes, in which squeezing is absent. What we can call *local squeezing* (i.e., squeezing in small regions of the transverse plane) can be obtained only in the presence of *spatially multimode squeezing*, (i.e., squeezing in a band of spatial modes). This has been predicted by Sokolov and Kolobov for a traveling-wave optical parametric amplifier (OPA) [6,7] and by our group for an optical parametric oscillator (OPO) [8,9]. Let us dwell a moment, for

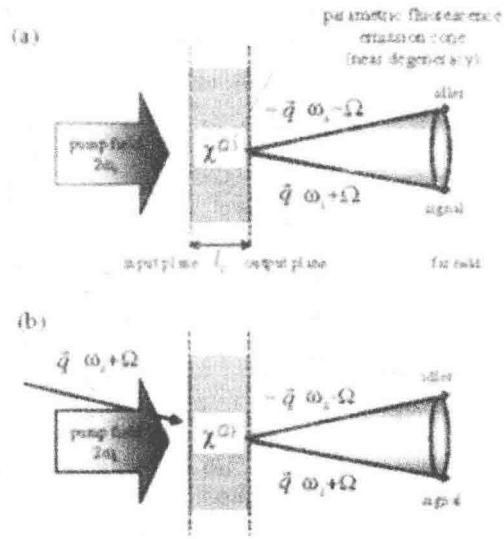

Fig. 1.5. (a) Scheme for parametric down-conversion of type-I. (b) Parametric amplification of a plane-wave; $\boldsymbol{q}$ is the component of the wave-vector in the plane orthogonal to the direction of propagation of the pump.

example, on the case of the OPA of type-I (Fig. 1.5a), in which one has a slab of $\chi^{(2)}$ material that is pumped by a coherent plane wave of frequency $2\omega_s$. A fraction of the pump photons is down-converted into signal–idler photon pairs, which are distributed over a broad band of temporal frequencies around the degenerate frequency ω_s. For each fixed temporal frequency, the

photon pairs are distributed over a band of spatial frequencies labeled by the transverse component $\boldsymbol{q}$ of the wave-vector.

If, in addition to the pump field, we inject a coherent plane wave with frequency $\omega_s + \Omega$ and the transverse wave-vector $\boldsymbol{q}$ (Fig. 1.5b), in the output we have a signal wave that corresponds to an amplified version of the input wave, and for this reason the system is called an optical parametric amplifier. Because of the pairwise emission of photons, there is also an idler wave that, close to degeneracy, is symmetrical with respect to the signal wave. Referring to the case in which only the pump is injected, two regimes can be distinguished. One is that of pure spontaneous parametric down-conversion, as in the case of a very thin crystal. In this case coincidences between partners of single photon pairs are detected. The other is that of dominant stimulated parametric down-conversion, in which a large number of photon pairs at a time is detected. In this chapter we will focus on the second case, whereas the first case will be considered in Chapter 2.

On a more formal ground, let us consider the down-converted signal–idler field emitted close to the degenerate frequency ω_s. Let us denote by $\hat{a}_{\rm in}(\boldsymbol{x}, t)$ the signal–idler complex amplitude envelope operator at the input endface of the crystal slab, and by $\hat{a}_{\rm out}(\boldsymbol{x}, t)$ the envelope operator at the output endface; t indicates time and $\boldsymbol{x} \equiv (x, y)$ is the coordinate vector in the endfaces. We expand $\hat{a}_{\rm in}$ and $\hat{a}_{\rm out}$ in Fourier modes in space and time:

$$\hat{a}_{\rm in}(\boldsymbol{x}, t) = \int \mathrm{d}\boldsymbol{q} \int \mathrm{d}\Omega \; \hat{a}_{\rm in}(\boldsymbol{q}, \Omega) \mathrm{e}^{\mathrm{i}\boldsymbol{q}\cdot\boldsymbol{x} - \mathrm{i}\Omega t} \,, \tag{1.27}$$

$$\hat{a}_{\rm out}(\boldsymbol{x}, t) = \int \mathrm{d}\boldsymbol{q} \int \mathrm{d}\Omega \; \hat{a}_{\rm out}(\boldsymbol{q}, \Omega) \mathrm{e}^{\mathrm{i}\boldsymbol{q}\cdot\boldsymbol{x} - \mathrm{i}\Omega t} \,. \tag{1.28}$$

One can demonstrate that, in the linear regime of an undepleted pump, the following input-output relations hold [9],

$$\hat{a}_{\rm out}(\boldsymbol{q}, \Omega) = U(\boldsymbol{q}, \Omega) \hat{a}_{\rm in}(\boldsymbol{q}, \Omega) + V(\boldsymbol{q}, \Omega) \hat{a}^{\dagger}_{\rm in}(-\boldsymbol{q}, -\Omega) \,, \tag{1.29}$$

$$\hat{a}_{\rm out}(-\boldsymbol{q}, -\Omega) = U(-\boldsymbol{q}, -\Omega) \hat{a}_{\rm in}(-\boldsymbol{q}, -\Omega) + V(-\boldsymbol{q}, -\Omega) \hat{a}^{\dagger}_{\rm in}(\boldsymbol{q}, \Omega) \,, \tag{1.30}$$

where the expressions of $U(\boldsymbol{q}, \Omega)$ and $V(\boldsymbol{q}, \Omega)$ are given in [9]. We can note immediately that, for each fixed $\boldsymbol{q}$, Ω, Eqs. (1.29) have the same form of the prototype model II (1.12). Hence the results of Section 1.2.2 hold for this case; for example, Fig. 1.5b corresponds to case 1 of Section 1.2.2. The case of parametric down-conversion of type-II will be considered in Chapter 5.

1.4.2 Near-Field/Far-Field Duality in Type-I OPAs

We want to illustrate the key spatial quantum properties of the field emitted by an OPA of type-I, in the linear regime of negligible pump depletion, or by an OPO below threshold.

In the near field (see Fig. 1.6) one has the phenomenon of spatially multimode squeezing or local squeezing discussed in Section 1.4.1. A good level of

squeezing is found, provided the region that is detected has a linear size not smaller than the inverse of the spatial bandwidth of emission in the Fourier plane. If, on the other hand, one looks at the far field (which can be reached, typically, by using a lens as shown in Fig. 1.6) one finds the phenomenon of *spatial entanglement* between small regions located symmetrically with respect to the center. Precisely, if one considers two symmetrical pixels 1 and 2 (Fig. 1.7a), the intensity fluctuations in the two pixels are very well correlated or, equivalently, the fluctuations in the intensity difference between the two pixels are very much below the shot-noise level [10, 11]. Precisely,

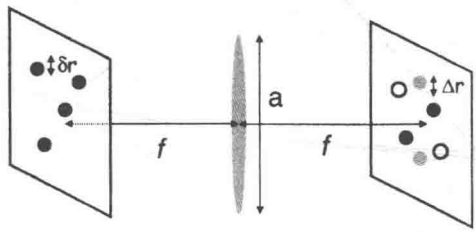

Fig. 1.6. Illustration of the near-field far-field duality; f is the focal plane of the lens. Not shown is the pump field of frequency $2\omega_s$ and the nonlinear slab.

let us consider the number of photons $\hat{N}_1$ and $\hat{N}_2$ detected in pixel 1 and 2, respectively, and the associated fluctuations $\delta\hat{N}_i = \hat{N}_i - \langle\hat{N}_i\rangle$ (i = 1, 2). For symmetry reasons one has that $\langle\hat{N}_1\rangle = \langle\hat{N}_2\rangle$, $\langle(\delta\hat{N}_1)^2\rangle = \langle(\delta\hat{N}_2)^2\rangle$. In the limit of the plane-wave pump, the photon number difference $\hat{N}_- = \hat{N}_1 - \hat{N}_2$ turns out to be fluctuationless [10]; that is,

$$\langle(\delta\hat{N}_-)^2\rangle = 0\,. \tag{1.31}$$

Basically, one has that $\hat{N}_1 = \hat{N}_2$; that is, by measuring $\hat{N}_1$ one can infer the value of $\hat{N}_2$ (entanglement). This result expresses in the most emphatic way the emission of signal and idler photons in pairs, and follows from the perfect correlation between the photons in 1 and 2. As a matter of fact one has

$$\langle(\delta\hat{N}_-)^2\rangle = \langle(\delta\hat{N}_1)^2\rangle + \langle(\delta\hat{N}_2)^2\rangle - 2\langle\delta\hat{N}_1\delta\hat{N}_2\rangle\,; \tag{1.32}$$

because $\langle(\delta\hat{N}_1)^2\rangle = \langle(\delta\hat{N}_2)^2\rangle$ one has from (1.31) that the normalized correlation

$$C \equiv \frac{\langle\delta\hat{N}_1\delta\hat{N}_2\rangle}{\sqrt{\langle(\delta\hat{N}_1)^2\rangle\langle(\delta\hat{N}_2)^2\rangle}} = 1\,, \tag{1.33}$$

which means perfect correlation. For the realistic case of a Gaussian pump, the fluctuations of $\hat{N}_-$ are below the shot-noise level; [10] that is

$$\langle(\delta\hat{N}_-)^2\rangle < \langle\hat{N}_+\rangle = \langle\hat{N}_1\rangle + \langle\hat{N}_2\rangle\,. \tag{1.34}$$

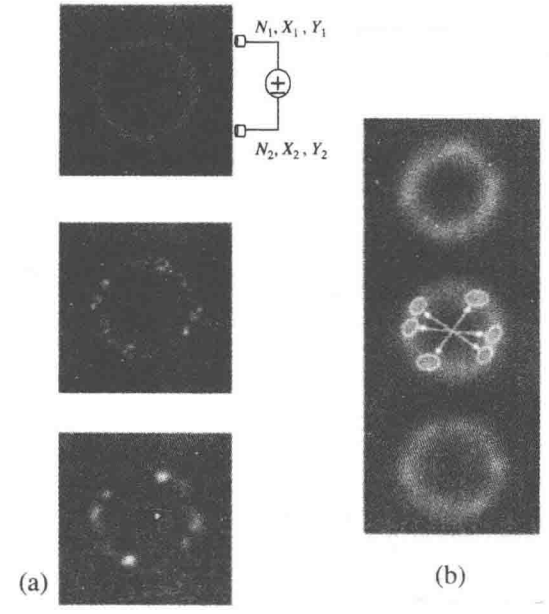

Fig. 1.7. Intensity distribution in the far field for a single shot of the pulsed pump field. (a) Numerical simulations. The waist of the pump beam is 1000 μm, 300 μm, 150 μm in the three frames from the top to the bottom, respectively. N_i, X_i, Y_i, (i = 1, 2) denote the photon numbers and the quadrature component measured in the two pixels 1 and 2, respectively. (b) Experimental observation by Devaux and Lantz at University of Besançon (see [13]).

Because this phenomenon arises for any pair of symmetrical pixels, we call it spatial entanglement. The same effect occurs also for quadrature components, because in the two pixels the fluctuations of the quadrature component $\hat{X}$ are almost exactly correlated, and those of the quadrature component $\hat{Y}$ are almost exactly anticorrelated [12]. The case of perfect correlation/anticorrelation occurs in the limit of the plane-wave pump, in which relations (1.21) hold.

The minimum size of the symmetrical small regions, among which one finds spatial entanglement, is determined by the finite aperture of optical elements, and is given, in the paraxial approximation, by $\lambda f/a$, where λ is the wavelength, f is the focal length of the lens and a is the aperture of optical elements (e.g., the lens aperture; Fig. 1.6). In a more realistic model of the OPA, the finite waist of the pump field must be taken into account. In this case the minimum size of the regions where entanglement is detectable in the far field is determined by the pump waist.

The spatial entanglement of intensity fluctuations in the far field is quite evident even in single shots (the pump field is typically pulsed). Figure 1.7a shows a numerical simulation in a case of noncollinear phase matching at the